AIAA JOURNAL
Vol. 30, No. 2, February 1992

Unsteady Pressure Field and Vorticity Production over a Pitching Airfoil

Mukund Acharya* and Metwally H. Metwally†
Illinois Institute of Technology, Chicago, Illinois 60616

The unsteady pressure field and the accompanying variations in the flux of spanwise vorticity from the surface were measured over a range of dimensionless pitch rates for a two-dimensional NACA 0012 airfoil model undergoing a single pitch-up motion. The results were examined to identify the mechanisms that play key roles in the initiation, development, growth, and movement of the dynamic-stall vortex. The unsteady pressure distribution over the airfoil was dominated by three features, whose emergence and evolution were used to distinguish between two classes of behavior, corresponding to low and high pitch rates. Further, it was found that the flux of vorticity from the surface originated primarily from five concentrated regions or sources, the majority of which were located over the forward portion of the airfoil surface. The behavior of vorticity flux from these sources was related to the interacting mechanisms responsible for the development of the flowfield. The change of these features in the pressure and surface vorticity flux variations with the pitch rate is described.

Nomenclature

c = airfoil chord
c_p = pressure coefficient, $(p - p_\infty)/\rho U_\infty^2/2$
p = static pressure
p_∞ = freestream static pressure
Re_c = Reynolds number based on chord, $U_\infty c/\nu$
S = surface vorticity flux, $\nu \partial u/\partial y$
S^+ = dimensionless vorticity flux, $2cS/U_\infty^2$
s = coordinate along airfoil surface
t = time
t_p = airfoil pitch time for angle $\Delta\alpha$
U_∞ = freestream velocity
x = chordwise location along airfoil (+ along suction surface and − along pressure surface)
y = coordinate normal to airfoil surface
α = airfoil angle of attack
α^+ = dimensionless pitch rate, $(\Delta\alpha c)/(t_p U_\infty)$
$\Delta\alpha$ = change in angle of attack
ν = kinematic viscosity
ρ = fluid density
ω = spanwise vorticity

Introduction

THE area of unsteady separated flow management has been receiving considerable attention in recent years. Depending on the application, the objectives of such flow management may be quite different. For instance, in the case of a highly maneuverable aircraft undergoing an unsteady pitch-up maneuver, the objective could be to utilize the increased dynamic lift obtained as a result of the formation of the dynamic-stall vortex without, however, allowing flow development to progress to a point where the vortex is shed from the airfoil suction surface with the accompanying undesirable effects of dynamic stall. In applications involving helicopter aerodynamics, the formation of the dynamic-stall vortex is undesirable altogether, and the objective of flow control could be to bleed the vorticity from the leading-edge region of the helicopter blade, thereby preventing vortex formation.

A successful system for the management of unsteady separation over airfoils must have two essential ingredients: the ability to identify the flow state reliably in real time in order to determine when control action needs to be initiated, and the availability of optimal flow controllers that can be activated when needed to modify the flow state in the desired manner. In addition, there are issues that need to be resolved in order to achieve the successful integration of these components into an active feedback control system. Accurate identification of flow state is tied strongly to a clear understanding of the unsteady production of vorticity and its detachment from the near-wall region. It is necessary to have a knowledge of the process by which vorticity is channeled into the dynamic-stall vortex, of the mechanisms that promote its growth and bind it to the forward region of the airfoil, and of the counteracting mechanisms that result in its movement over the suction surface and cause its ultimate detachment from the airfoil. Such an understanding, coupled with the establishment of a vorticity balance and a knowledge of the time scales of the evolutionary process, are prerequisites for the development of suitable on-line or reactive control techniques.

Background

An extensive body of work (McCroskey,[1] Gad-el-Hak,[2] and Ericsson and Reding[3] provide good reviews) has been reported in recent years describing experiments that examined the unsteady flow over two-dimensional airfoil models undergoing prescribed pitching motions. These studies were largely motivated by the need to understand helicopter blade aerodynamics and, more recently, by interest in aircraft supermaneuverability. The bulk of these investigations focused their attention on obtaining an understanding of dynamic stall and the influence of parameters such as airfoil geometry, Reynolds number, oscillation amplitudes, and rates. A few computational studies of the problem have also been carried out; among the more recent is that by Visbal and Shang.[4] Although knowledge of this phenomenon has improved considerably,[5,6] the physical mechanisms that play fundamental roles in the initiation, development, growth, movement, and detachment of the dynamic-stall vortex are still not understood completely. In addition, if flow control measures are to be effective, the behavior of the flow in the early stages of the evolution of the

Presented as Paper 90-1472 at the AIAA 21st Fluid Dynamics, Plasma Dynamics, and Lasers Conference, June 18-20, 1990, Seattle, WA; received July 5, 1990; revision received April 30, 1991; accepted for publication May 2, 1991.

*Associate Professor, Fluid Dynamics Research Center. Member AIAA.
†Graduate Research Assistant, Fluid Dynamics Research Center.

dynamic-stall vortex needs to be examined carefully, and the mechanisms responsible for this evolution process need to be understood well.

Some work has also been reported on the problem of flow-state detection. In an investigation of a generic, unsteady separating flow, Ramiz and Acharya[7] showed that relatively simple techniques involving measurements of the wall static pressure may be used to obtain reliable indicators of flow state. In these experiments, an unsteady separation was introduced in a boundary layer by the motion of a separation generator (a spanwise flap) into the flow. Phase-conditioned measurements of the time-varying flow direction, at various locations downstream of the flap, and the corresponding wall pressure data were used to track the separation as it developed. A number of possible criteria for flow-state identification, based on the unsteady wall-pressure measurements, were investigated, and two techniques were shown to have good promise. One of these was based on a comparison of the wall-pressure signature with a preset threshold, whereas the other involved an examination of the time derivative of the pressure signal. Although the specific criteria developed for this model flow may not be applicable to unsteady separation over any general configuration, the work established that measurements of the wall static pressure can be used to obtain reliable, real-time indications of the onset of separation and of the state of flow. Any practical flow-management system must depend on such simple, yet effective, measurements.

Objectives

The overall objective of the present work is to develop techniques for the control and management of separated flows over airfoils, particularly under unsteady operating conditions. The results are expected to help achieve the ultimate goal, which is the development of flow-management systems for highly maneuverable aircraft.

The present paper describes the first phase of this effort, in which the evolution of the dynamic-stall vortex has been studied to gain an improved understanding of the mechanisms relevant to this process. The results of this phase are being used to develop reliable ways to identify the flow state over the airfoil during its motion as well as to develop techniques of flow control that could be used to alter the flow development in the manner desired.

Experimental Arrangement

Wind Tunnel

The experiments were conducted in the Andrew Fejer Unsteady Flow Wind Tunnel at Illinois Institute of Technology. This is a closed-circuit, low-speed facility, with a test section 0.6 × 0.6 m in cross section and 3.1 m in length. Flow velocities up to 40 m/s can be obtained in this facility, with a corresponding freestream turbulence level of 0.03%. Special features of this wind tunnel include the ability to introduce a controlled oscillation in the flow, using a computer-controlled shutter mechanism mounted at the downstream end of the test section, as well as provisions to impart a prescribed motion to a model positioned in the flow. The latter feature was used in the present experiments.

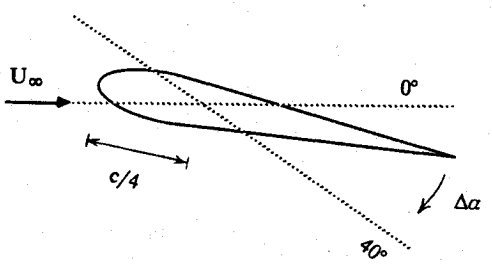

Fig. 1 Experimental arrangement.

Airfoil Model

An airfoil model with a NACA 0012 profile, a chord length of 30 cm, and a span of 60 cm was used. It was mounted in the horizontal midplane of the test section, allowing it to be pitched about its quarter-chord line, as shown schematically in Fig. 1. The motion of the airfoil was derived from a low-inertia, high-torque, printed-circuit, servo-controlled dc motor, driven using an IBM AT-compatible personal computer and a programmable digital-to-analog interface. A rotary variable differential transformer (RVDT) was used to obtain a signal indicative of the airfoil angle of attack.

The airfoil was instrumented with a total of 24 static-pressure ports. Of these, 21 were in the central plane of the model, with 1 on the nose and the remaining 20 distributed over the upper surface. Two of the three additional ports were positioned at ±10 cm from the centerline, at 26% chord, to check for three-dimensional effects. The third was located on the centerline of the lower surface, at a chordwise location of 1.7%. This last port was used together with the corresponding port on the upper surface to align the airfoil with respect to the flow direction. A key feature of the model design and the port locations was the spatial resolution obtained in the pressure measurements in the leading-edge region of the airfoil. A total of nine pressure ports were located between the nose of the airfoil and 14% chord at 0, 0.8, 1.7, 3.2, 4.6, 6.1, 7.5, 10.6, and 13.8% chord. As discussed later in this paper, this spatial resolution proved to be essential in understanding the unsteady flow behavior. The pressure ports were connected with tubing of equal lengths to a Scanivalve placed inside the airfoil. The Scanivalve enabled connection of any one of the ports to the pressure transducer described below. Pressure information over the suction or pressure surface was obtained by pitching the airfoil either up or down, respectively.

Instrumentation

A model 239 Setra differential pressure transducer was used in conjunction with the Scanivalve system for the pressure measurements. The overall, uncompensated response of the system, including the pressure transducer, Scanivalve, and tubing, was within 3 dB up to a frequency of 50 Hz. This value was adequate for the present experiments.

A Masscomp MC5500 computer system was used for all of the data acquisition and processing.

Measurements

For the experiments described in this paper, a single, constant-velocity, hold-pitch-hold motion of the airfoil was used where the time-motion history of the model was described by the ramp function in Fig. 2. The initial and final angles were 0 and 40 deg, respectively, and the approach flow velocity was varied between 4.3 and 5.7 m/s, whereas the pitch time t_p was varied between 0.1 and 1.0 s. The unsteady flow development over the airfoil was studied for a chord Reynolds number range $8.8 \times 10^4 \leq Re_c \leq 1.2 \times 10^5$, and a dimensionless pitch rate $0.036 \leq \alpha^+ \leq 0.77$. This paper describes measurements of the unsteady surface pressure and surface vorticity flux variations over the airfoil. A complete discussion of all of the measurements, including vertical and horizontal smoke-wire visualization studies, is given by Metwally.[8] A wide range of dimensionless pitch rates was covered in the study, encompassing the typical ranges encountered for helicopter rotors and highly maneuverable aircraft and extending this range to higher values in order to examine the trends in

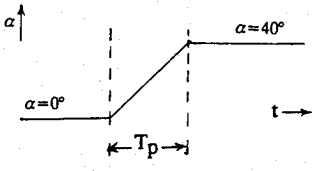

Fig. 2 Time-motion history for pitch-up of the airfoil.

unsteady-flow behavior. The pitch rate and Reynolds number were not varied independently. The Reynolds number range covered was low compared to that found in practical situations, and the flow was essentially incompressible. However, as discussed in Ref. 8, the dominant parameter controlling the unsteady effects described in this paper is the pitch rate; Reynolds number and compressiblity effects are secondary. The important physical aspects of the flow development can be understood from experimental studies in this lower Reynolds number regime since many of the key features of the dynamics are common to a wider range of Reynolds number. Other work[9] also substantiates this conclusion.

Results

Unsteady Pressure Measurements

The variation of pressure over the suction and pressure surfaces during the pitch-up of the airfoil was examined in detail for five values of the dimensionless pitch rate α^+: 0.036, 0.072, 0.18, 0.36, and 0.49. The procedure adopted for these measurements was as follows. The static pressure at a selected port on the airfoil surface was recorded, together with the airfoil position signal, during the pitch-up motion of the airfoil. Five such realizations of this pressure-time history were obtained, and an ensemble average computed. This procedure was repeated for each of the pressure ports, and the ensemble-averaged data were aligned and cross plotted to obtain the chordwise pressure distribution over the suction surface at successive incremental angles during the pitch-up of the airfoil. An identical procedure, with the airfoil pitching down, was used to obtain the pressure-surface data.

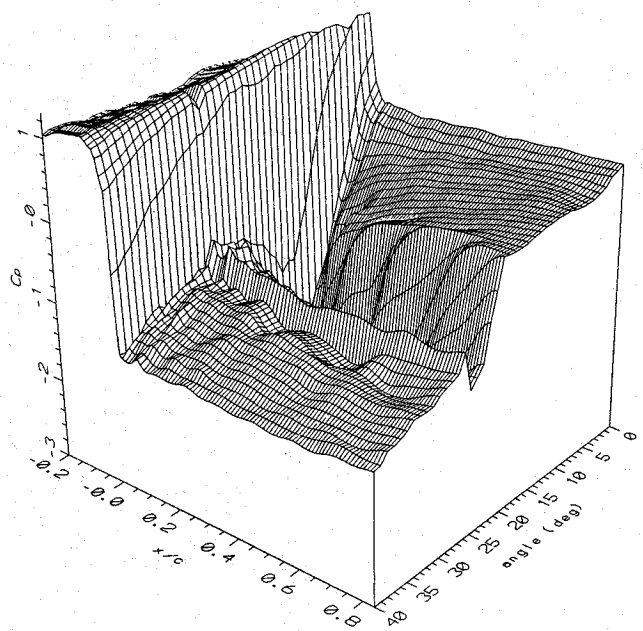

a) $\alpha^+ = 0.036$

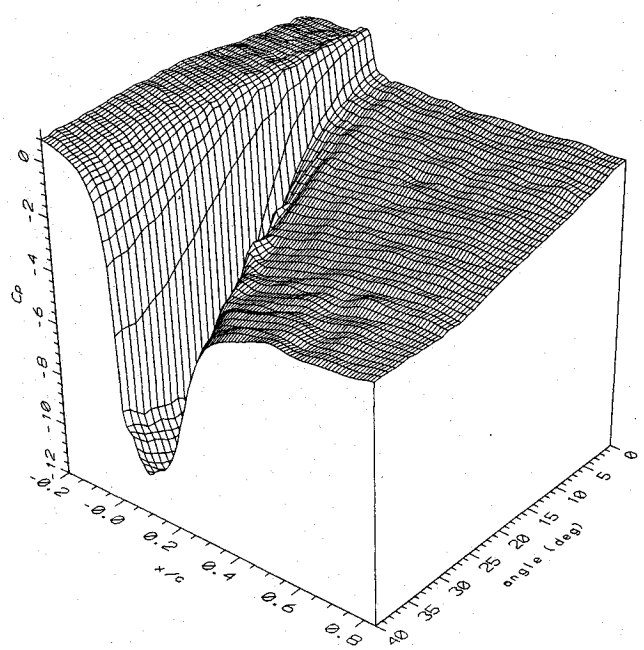

b) $\alpha^+ = 0.49$

Fig. 3 Pressure variation over suction surface during pitch-up.

Figures 3 show the pressure variation over the suction surface during the pitch-up for α^+ of 0.036 and 0.49, values that are characteristic of two classes of behavior corresponding to low and high pitch rates, respectively. Shown plotted for each case is the variation of the pressure coefficient c_p over the suction surface for angles between 0 and 40 deg. A careful examination of the individual traces that make up these figures revealed three dominant features: a suction peak in the region close to the leading edge (LESP), a constant pressure region or pressure plateau (CPP), and a suction peak associated with the dynamic stall vortex (DSVP). The CPP is related to a region of unsteady reversed flow that forms downchord of the LESP. In a strict sense, this region is not the same as the laminar separation bubble seen over stationary airfoils at angles of attack; it is the result of the unsteady shear layer that separates from the airfoil suction surface in the near-leading-edge region as the airfoil pitches up. The characteristics that distinguish the two classes of behavior are related to the emergence and subse-

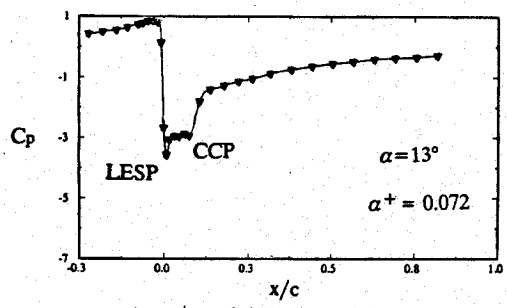

a) $\alpha^+ = 0.072$, $\alpha = 13$ deg

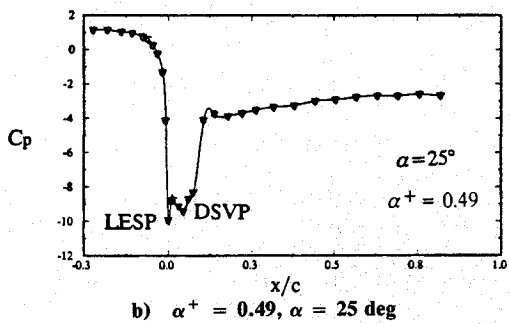

b) $\alpha^+ = 0.49$, $\alpha = 25$ deg

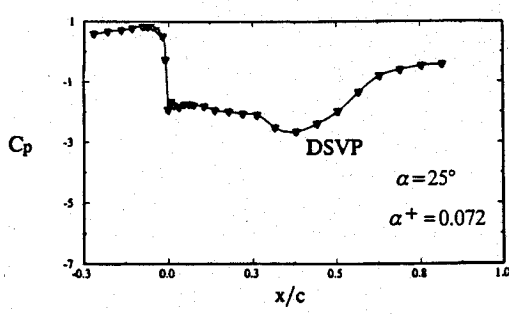

c) $\alpha^+ = 0.072$, $\alpha = 25$ deg

Fig. 4 Typical pressure variations over the suction and pressure surface.

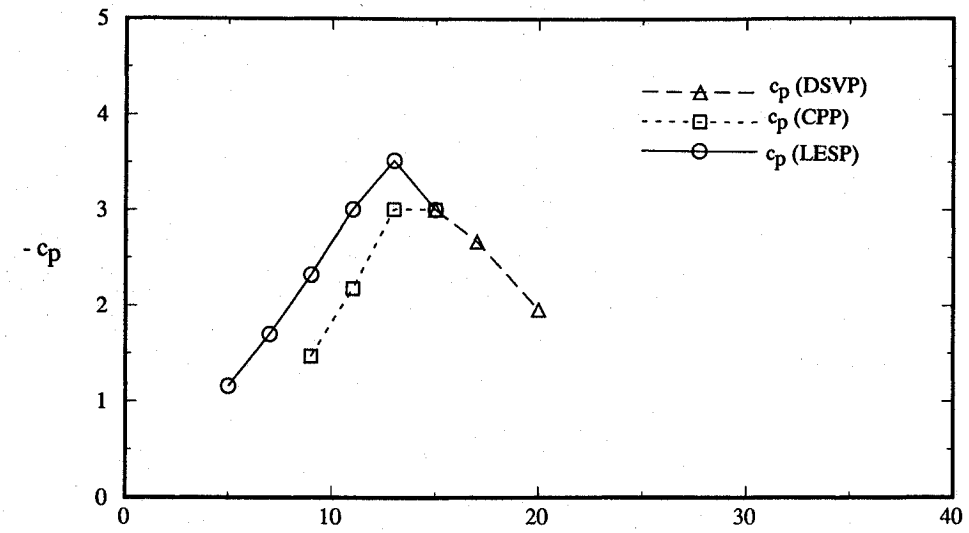

a) $\alpha^+ = 0.036$

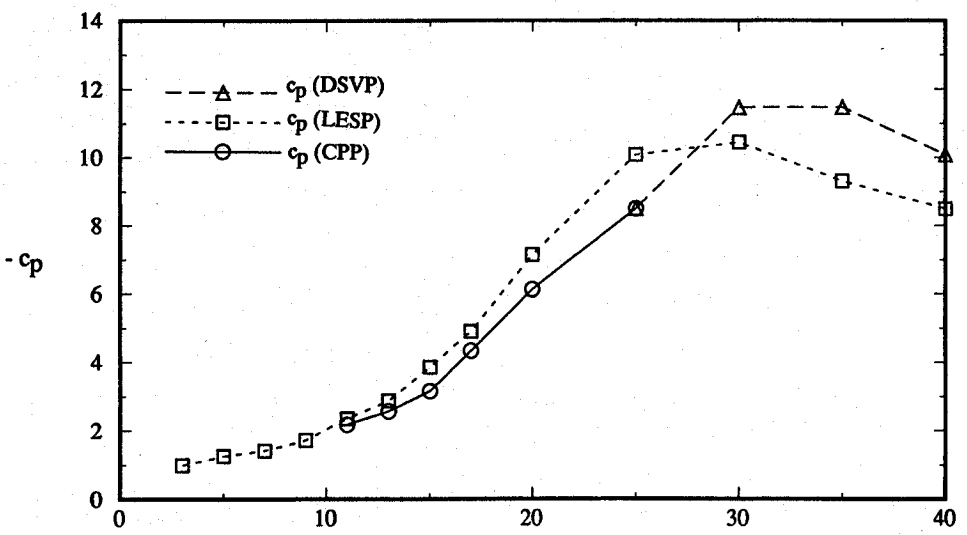

b) $\alpha^+ = 0.49$

Fig. 5 Variation of c_p associated with dominant features in the pressure distribution.

quent behavior of these three features: the LESP, CPP, and DSVP. The details of these features are not easily seen in the composite pressure plots of Figs. 3, but are revealed in the typical individual traces at different angles shown in Figs. 4. These traces were extended to include the pressure variation over the first 30% of the pressure surface. Locations along the pressure surface are indicated by a negative value of x/c.

For both classes of behavior, the pressure distribution over the suction surface during the initial stages of pitch up is characterized by the formation of the LESP within the first 1% of chord (Fig. 4a). The magnitude of the section peak increases as the airfoil pitches up, and the peak moves closer in toward the nose of the airfoil (Fig. 4b). Some time after the formation of the peak, the CPP appears just downchord of the LESP, within the first 10% of chord (Fig. 4a). As the airfoil motion progresses, the magnitude of the suction pressure associated with this pressure plateau also increases. Beyond this state, the flow development associated with the two classes of behavior is different.

At low pitch rates (class A), the magnitude of suction pressure asssociated with the LESP and CPP increase up to a point when they are the same. The LESP is then, for all practical purposes, no longer distinguishable from the CPP. The CPP region deforms into the DSVP and opens up or spreads rapidly along the surface, resulting in the spilling, or movement and subsequent detachment of the dynamic stall vortex, off the airfoil. The magnitudes of the suction pressure associated with the DSVP are rather small in comparison to those of class B.

At high pitch rates (class B), the CPP region deforms into the suction peak that is characteristic of the dynamic stall vortex (DSVP), as seen in Fig. 4b. This deformation occurs before the levels of pressure in the LESP and CPP reach the same magnitude. The vortex remains compact and stays positioned over the forward region of the airfoil (within the first 10% of chord). At the same time, the magnitude of pressure of the LESP increases further while the peak moves right up to the nose of the airfoil. There are thus two distinct suction peaks that coexist over the suction surface for a period of time. At a later stage in the airfoil motion, the magnitude of the pressure associated with the LESP starts to decrease and, simultaneously, the dynamic-stall vortex begins to grow in extent and move down chord, as evidenced by the broadening and movement of the DSVP (Fig. 4c).

The DSVP is clearly evident in Fig. 3b. At these high pitch rates, the vortex is still stationed over the airfoil surface at the end of the motion, whereas at pitch rates such as those of Fig.

3a, the vortex has grown in extent and shed by the time the motion is completed.

Figures 3 and 4 show typical examples of data in order to describe the significant features in the development of the pressure field over the airfoil. These three features were seen for all of the values of α^+ studied and were tracked during the pitch-up of the airfoil. The value of the pressure coefficient associated with each feature (the *maximum* value for LESP and DSVP and the *level* for CPP), as well as the change in location of the feature over the airfoil surface, were determined for different angles of attack during the pitch-up. Figures 5 show the variation of the pressure coefficient for each of these features, with angle of attack, during the pitch-up for typical cases, $\alpha^+ = 0.036$ and 0.49. These plots support the previous description of the two classes of behavior. In this figure, lines have been drawn through the data points in order to aid in viewing the plots.

The simultaneous existence of the two strong suction peaks and the related hold time of the dynamic-stall vortex over the forward region of the airfoil are two significant characteristics that distinguish these two classes of behavior. The transition from one class of behavior to the other with a change in α^+ is illustrated in Fig. 6. Here, the initial and final angles at which the LESP was seen in the pressure profiles, as well as those at which the DSVP was detected, are shown plotted in $\alpha^+ - \alpha$ space. For values of $\alpha^+ > 0.1$, the two features coexist in the forward region of the airfoil. The continued presence of a strong LESP allows the dynamic-stall vortex to be held in this region for progressively larger angles of attack as α^+ increases. The mechanisms responsible for these two classes of behavior can be understood better by examining the flux of vorticity from the surface of the airfoil into the flow.

Flux of Vorticity from the Airfoil Surface

The approach flow is essentially irrotational; the airfoil surface is the only source of vorticity for the flowfield. The motion of the surface and the flow events within the viscous region are strongly coupled; the unsteady separation process and the related sequence of events discussed earlier are strongly affected by the vorticity generated at the wall. In their review paper, Reynolds and Carr[10] showed that for both steady and unsteady flows the rate of vorticity generation at the surface, that is, the flux of spanwise vorticity ω from the surface, is related to three quantities: the instantaneous streamwise pressure gradient, the vorticity transported by transpiration through the surface, and the tangential acceleration of the surface. For constant velocity motion of the airfoil, and in the absence of transpiration, the last two effects make no contribution, and the flux of vorticity from the surface is given by

$$S = \frac{1}{\rho}\frac{\partial p}{\partial s}$$

The behavior of the surface vorticity flux over the airfoil during the motion was determined for each of the cases studied, from this equation, by using spline fits to the ensemble-averaged pressure data described in the previous section. Care was taken to ensure that this procedure did not introduce any artificial variations in the data. Different spline tensions were tried; in addition, spline fits to individual realizations were also processed and compared with the results for the ensemble-averaged data. This procedure established that the features in the surface vorticity flux, described later, were real and not a result of the data processing.

Figures 7 show the variation of the dimensionless surface vorticity flux S^+ over the suction surface at different angles

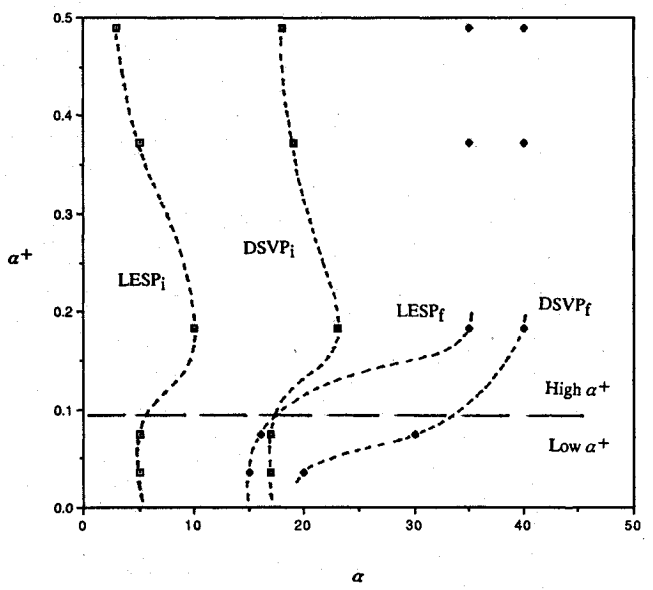

Fig. 6 Transition from class A to class B behavior with change in α^+.

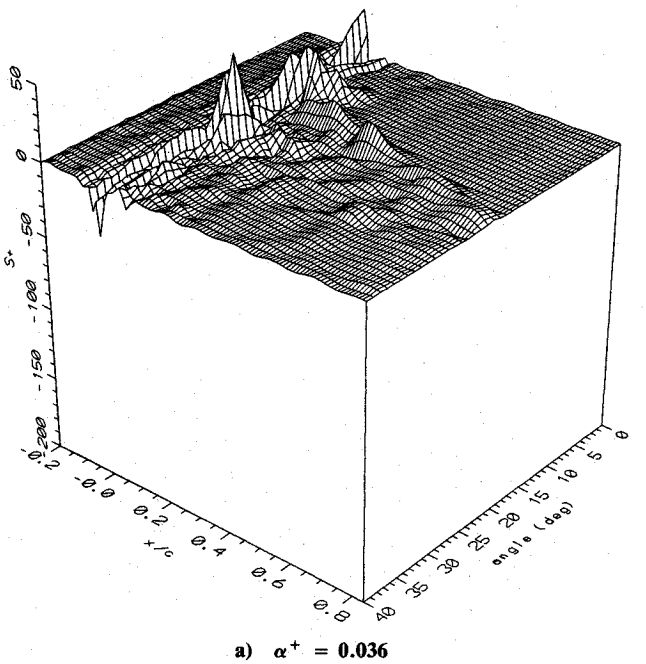

a) $\alpha^+ = 0.036$

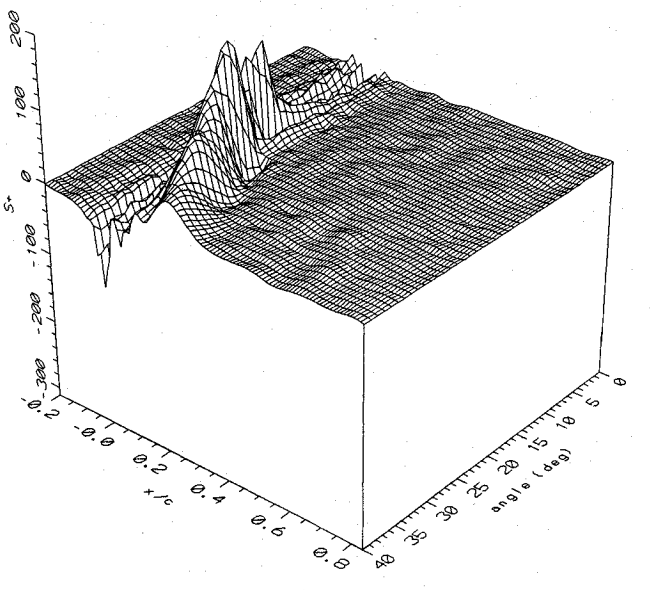

b) $\alpha^+ = 0.49$

Fig. 7 Surface vorticity flux variations over suction surface during pitch-up.

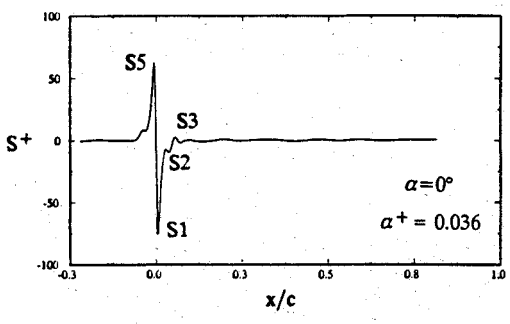

a) $\alpha^+ = 0.036$, $\alpha = 0$ deg

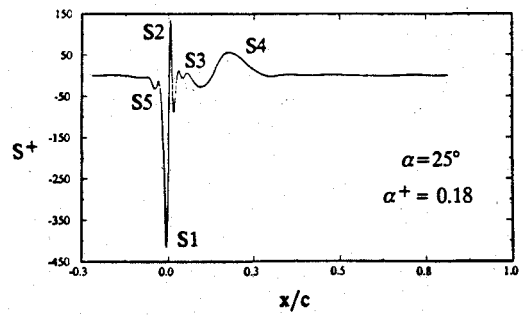

b) $\alpha^+ = 0.18$, $\alpha = 25$ deg

Fig. 8 Typical surface vorticity flux variations over the suction and pressure surfaces.

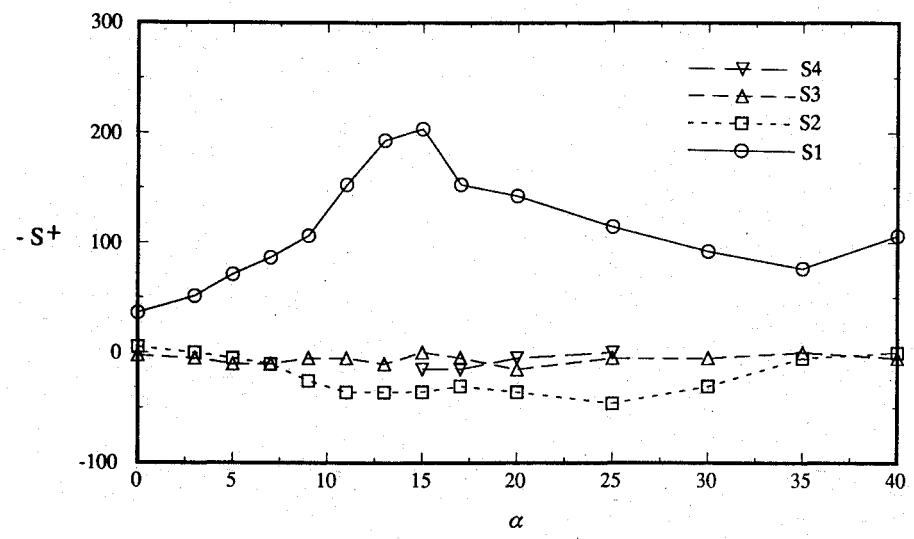

a) $\alpha^+ = 0.036$

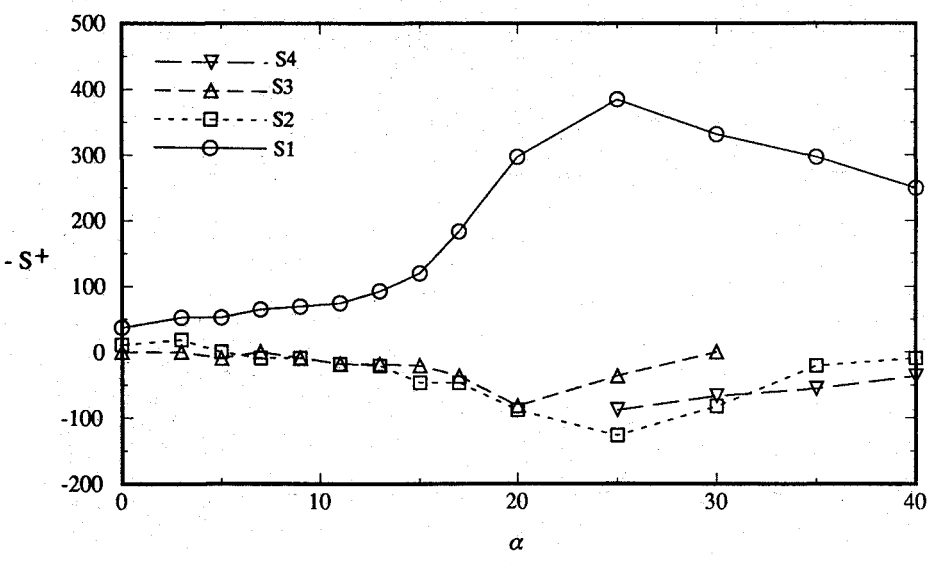

b) $\alpha^+ = 0.49$

Fig. 9 Variation of surface vorticity flux associated with the characteristic peaks.

during the motion of the airfoil for the two classes of behavior discussed earlier. The first notable observation is that, apart from the flux associated with the dynamic-stall vortex as it moves downchord, the vorticity is introduced into the flow primarily from a region of the surface in the neighborhood of the leading edge, within the first 10% of the chord. An examination of the individual traces at different angles showed further that in all the cases the bulk of this vorticity flux was concentrated in five characteristic peaks with very little contribution from other locations on the surface. Figures 8a and 8b show two typical chordwise variations of the surface vorticity flux with these characteristic peaks labeled *S1–S5*. To a very good approximation, the flux of vorticity from the surface may be modeled as originating from five concentrated sources, associated with these peaks, that move about the airfoil surface during the airfoil motion. As with the dominant features of the pressure distribution, these peaks were tracked during the pitch-up of the airfoil for the five values of α^+. The

value of S^+ at each peak and the position of each peak over the airfoil surface were determined. This information is shown plotted in Figs. 9 and 10 for the two typical cases $\alpha^+ = 0.036$ and 0.49, respectively. Also shown in Figs. 10 is the change in location of the three features in the pressure field, described in Figs. 5, and the movement of the stagnation point down the pressure surface of the airfoil. Lines have been drawn through the data points in Figs. 9 and 10 to aid in viewing these plots.

The two most important features are the peaks labeled *S*1 and *S*2. *S*1 is a source of negative (clockwise) vorticity and is responsible for most of the vorticity that is channeled in to the dynamic-stall vortex. As seen in Figs. 9, the magnitude of *S*1 increases rapidly as the airfoil pitches up, reaches a maximum, and then drops rapidly. The location of this peak, shown in Figs. 10, moves from a point on the suction surface, around the nose of the airfoil, to the pressure side of the airfoil before the rapid increase in the peak magnitude begins. The peak remains at all times within 1% of chord in either side of the nose. Thus, the primary source of vorticity for the dynamic-stall vortex is this very small region of the airfoil surface in the neighborhood of the nose of the airfoil. Lines have been drawn through the data points in Figs. 9 and 10 to aid in viewing these plots.

The peak *S*2 is a source of positive or clockwise vorticity, located initially at around 3% of chord on the suction surface and then moving in toward the nose to a position between 0.5 and 1% of chord. A look at Figs. 5, 9, and 10 shows that the rapid increase in the magnitude of *S*2, the rapid decrease in the magnitude of *S*1 after it has peaked, and the initiation of rapid movement of the dynamic-stall vortex down the suction surface are all strongly correlated.

Although the measurements reported here do not reveal any direct evidence of its existence, we believe that the counter-clockwise vorticity from *S*2 is channeled into a counter-rotating vortex that forms over the suction surface between 1 and 2% of chord. We are presently carrying out flow-visualization experiments to confirm this hypothesis. Negative vorticity from *S*1 continues to be fed into the dynamic-stall vortex in a sheet moving over and around this counter-rotating vortex. It appears from the present measurements that the rapid rise in magnitude of *S*2 increases the strength of this vortex, which then moves to cut off the dynamic-stall vortex from its source of vorticity. The rapid growth and movement of the dynamic-stall vortex is initiated after this event. This picture is consistent with the process of breakaway or eruption that has been observed by Smith and Walker[11] and others.

Another interesting observation from these measurements is the increase in the magnitude of the peak value attained by *S*1, with increasing pitch rate, shown plotted in Figs. 11, together with the location of *S*1 when the peak value is reached. With increasing α^+, the amount of vorticity that is fed into the dynamic stall vortex increases. In addition, this accumulation occurs over a smaller period of time. The combination of these two factors results in the formation of a vortex that is more compact and of increased strength as the pitch rate is increased.

The other peaks, *S*3, *S*4, and *S*5, do not make a strong contribution to the evolution of the flow, as described earlier. Initially, *S*5 is the source that feeds boundary-layer sign vorticity

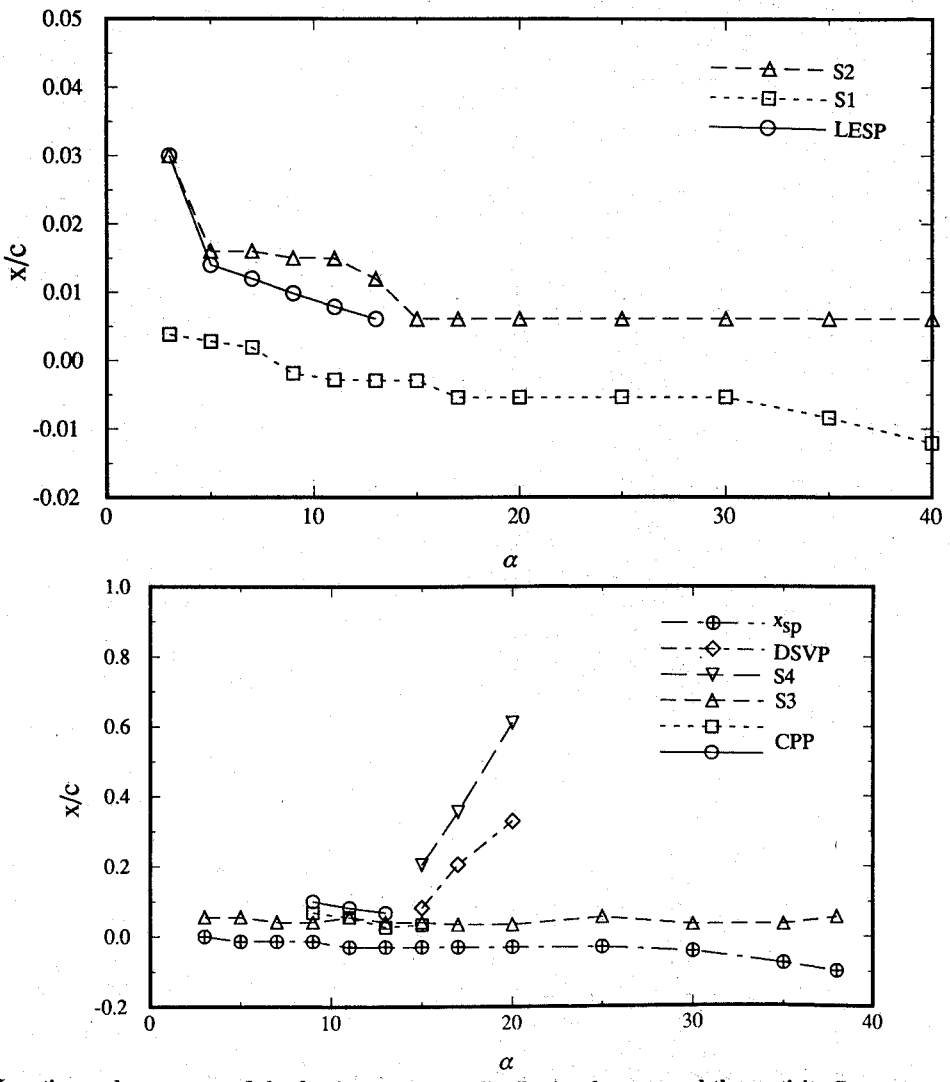

Fig. 10a Location and movement of the dominant pressure-distribution features and the vorticity flux peaks, $\alpha^+ = 0.036$.

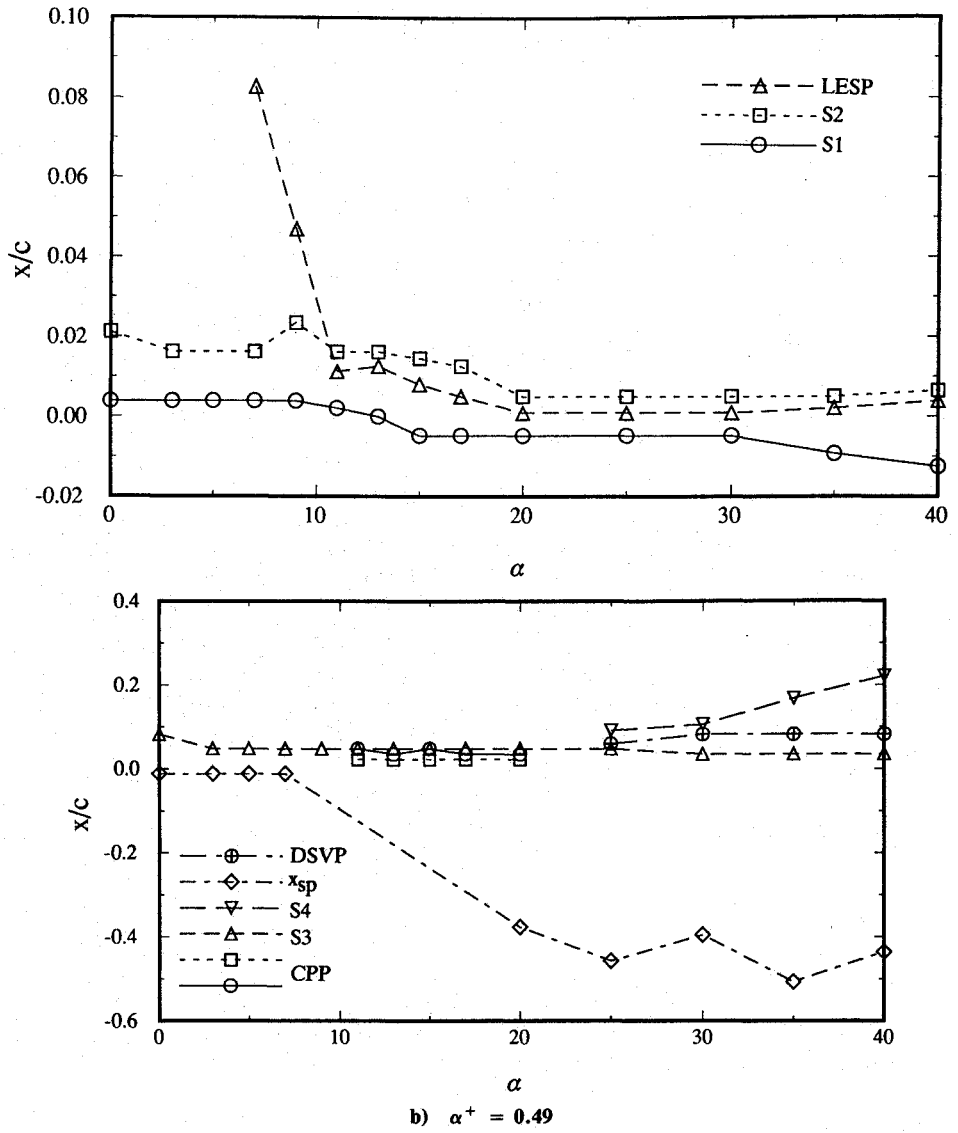

b) $\alpha^+ = 0.49$

Fig. 10b Location and movement of the dominant pressure-distribution features and the vorticity flux peaks, $\alpha^+ = 0.49$.

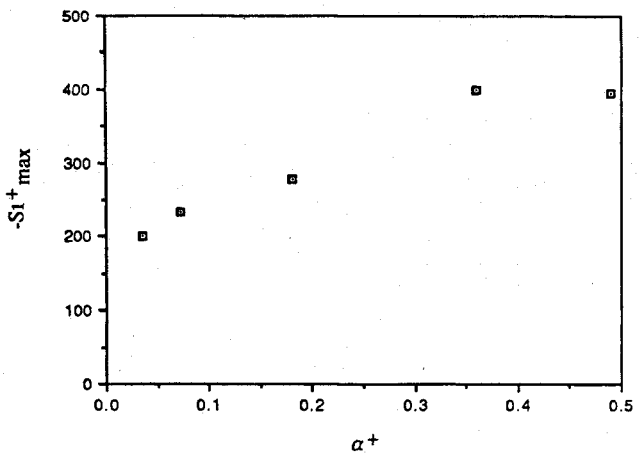

Fig. 11a Variation of maximum value of *S*1 with pitch rate.

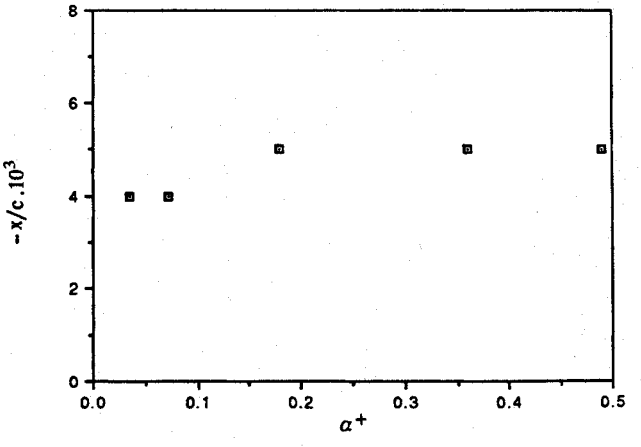

Fig. 11b Variation of location of maximum value of *S*1 with pitch rate.

into the flow on the pressure side of the airfoil. As the airfoil pitches up, the stagnation point moves down the pressure side from the nose, past this location, and the magnitude of this peak becomes very small in comparison to *S*1. As mentioned earlier, *S*4 is a peak that forms as a consequence of the motion of the dynamic-stall vortex down the suction surface, whereas *S*3 is a secondary source of counterclockwise vorticity, further down chord from *S*2 (between 5 and 10% of chord), that is always smaller in comparison to *S*2, although it grows somewhat in magnitude with increasing pitch rate.

Conclusions

Measurements of the pressure distribution over the airfoil model and the variations in the flux of surface vorticity during the pitch-up have helped bring about an increased understanding of the mechanisms that interact to control the evolution of this complex unsteady flow. A significant feature of these data was the spatial resolution in the forward portion of the airfoil surface that allowed the details of these variations to be captured. The process by which the dynamic-stall vortex forms, grows, and detaches from the suction surface has been identified. The results have also provided a sound basis for the development of procedures that might be adopted in a successful unsteady-flow management system. The requirements for such procedures are being investigated and will be described in a subsequent paper.

Acknowledgments

This work was carried out with the sponsorship of the Air Force Office of Scientific Research, under Grant 90-0173, monitored by H. Helin. We thank the reviewers for their constructive comments.

References

[1]McCroskey, W. J., "Unsteady Airfoils," *Annual Review of Fluid Mechanics,* Vol. 14, 1982, pp. 285–311.

[2]Gad-el-Hak, M., "Unsteady Separation on Lifting Surfaces," *Applied Mechanics Review,* Vol. 40, 1987, pp. 441–452.

[3]Ericcson, L. E., and Reding, J. P., "Fluid Dynamics of Unsteady Separated Flow. Part II. Lifting Surfaces," *Progress in Aerospace Sciences,* Vol. 24, 1987, pp. 249–356.

[4]Visbal, M. R., and Shang, J. S., "Investigation of the Flow Structure Around a Rapidly Pitching Airfoil," *AIAA Journal,* Vol. 27, No. 8, 1989, pp. 1044–1051.

[5]Robinson, M. (ed.), *Proceedings of the Second Workshop on Unsteady Separated Flows,* USAF Academy, Colorado Springs, 1988.

[6]Carr, L. W. (ed.), *Proceedings of the NASA/AFOSR/ARO Workshop on the Physics of Forced Unsteady Separation,* NASA Ames Research Center, Moffett Field, CA, 1990.

[7]Ramiz, M. A., and Acharya, M., "Detection of Flow State in an Unsteady Separating Flow," *AIAA Journal,* Vol. 30, No. 1, 1992, pp. 117–123.

[8]Metwally, M. H., "Investigation and Control of the Flow Field over a Pitching Airfoil," Ph.D. Dissertation, Mechanical and Aerospace Engineering Department, Illinois Institute of Technology, Chicago, IL, Dec. 1990.

[9]Visbal, M. R., "On Some Physical Aspects of Airfoil Dynamics Stall," ASME Symposium on Non-Steady Fluid Dynamics, Toronto, Canada, 1990.

[10]Reynolds, W. C., and Carr, L. W., "Review of Unsteady, Driven, Separated Flows," AIAA Paper 85-0527, March 1985.

[11]Smith, C. R., and Walker, J. D. A., "Some Aspects of Unsteady Separation," *Proceedings of the NASA/AFOSR/ARO Workshop on the Physics of Forced Unsteady Separation,* NASA Ames Research Center, Moffett Field, CA, 1990.